Original research

Cultivar discrimination of litchi fruit images using deep learning

Yutaro Osako[1], Hisayo Yamane[1], Shu-Yen Lin[2], Po-An Chen[3], Ryutaro Tao[1]

[1]Graduate School of Agriculture, Kyoto University, Kyoto, Japan

[2]Department of Horticulture and Landscape, National Taiwan University, Taipei, Taiwan

[3]Plant Technology Laboratories, Agricultural Technology Research Institute, Hsinchu, Taiwan

Corresponding author

Hisayo Yamane

hyamane@kais.kyoto-u.ac.jp

Laboratory of Pomology, Graduate School of Agriculture, Kyoto University, Kyoto 606-8502, Japan

ABSTRACT

Litchi (*Litchi chinensis* Sonn.) originated from China and many of its cultivars have been produced in China so far during the long history of cultivation. One problem in litchi production and research is the worldwide confusion regarding litchi cultivar nomenclature. Because litchi cultivars can be described in terms of cultivar-dependent fruit appearance, it should be possible to discriminate cultivars of postharvest fruits. In this study, we explored this possibility using recently developed deep learning technology for four common Taiwanese cultivars ‘Gui Wei’, ‘Hei Ye’, ‘No Mai Tsz’, and ‘Yu Her Pau’. First, we quantitatively evaluated litchi fruit shapes using elliptic Fourier descriptors and characterized the relationship between cultivars and fruit shapes. Results suggest that ‘Yu Her Pau’ can be clearly discriminated from others mainly based on its higher length-to-diameter ratio. We then fine-tuned a pre-trained VGG16 to construct a cultivar discrimination model. Relatively few images were sufficient to train the model to classify fruit images with 98.33% accuracy. We evaluated our model using images of fruits collected in different seasons and locations and found the model could identify ‘Yu Her Pau’ fruits with 100% accuracy and ‘Hei Ye’ fruits with 84% accuracy. A Grad-CAM visualization reveals that this model uses different cultivar-dependent regions for cultivar recognition. Overall, this study suggests that deep learning can be used to discriminate

litchi cultivars from images of the fruit.

Keywords:

Convolutional neural network, Deep learning, Image recognition, Litchi, Lychee, Machine learning, Fruit shape

1. Introduction

Litchi (*Litchi chinensis* Sonn.) is a subtropical fruit tree species that belongs to Sapindaceae. It originated in the region between southern China, northern Vietnam, and Myanmar (Mitra and Pathak, 2010). ~~China has the longest history of litchi cultivation, which was confined to southern China and possibly northern Vietnam until the late 17th century. Litchi cultivation then spread to other Asian countries such as Myanmar, India, Nepal, Bangladesh, Thailand, the Philippines, and Indonesia (Huang et al., 2005). From the 1800s to 1900s, litchis were introduced to other regions around the world such as South Africa, Australia, North America, South America, and Israel (Huang et al., 2005)~~. China accounts for nearly 80% of the global plantings, with production concentrated in the Guangdong, Guangxi, Fujian, and Hainan provinces. In China, over 200 cultivars, lines, or individuals with unique features have been identified so far (Wu, 1998). Nearly all the cultivars grown throughout the world originated in China, although artificial cross breeding programs have recently begun in some countries (Huang et al., 2005). Litchi was introduced to Taiwan from the Fujian Province of China nearly 300 years ago and commercial cultivation started in the 1950s (Chang, 1961). Commercial cultivation rapidly increased in Taiwan and reached a peak production with 14,682 ha of production area in 1988, and then declined (Chang et al., 2005). In Taiwan, litchi is an important fruit crop after citrus, mango, and pineapple (Taiwan Agricultural Statistic Year Book, 2015). In Taiwan, more than 30 cultivars have been reported to be under cultivation, and a few cultivars are under large-scale commercial production (Chang et al., 2009). 'Hei Ye' ('Haak Yip' or 'Black leaf'), 'Yu Her Pau' ('Fei Zi Xiao' or 'Fay Zee Siu'), and 'No Mai Tsz' are the top three cultivars in Taiwan (Chang et al., 2017).

One problem in litchi production and research is that there is worldwide confusion regarding litchi cultivar nomenclature. Different names are assigned to the same cultivar (synonyms) and the same (or similar) names are used for different cultivars (homonyms). These confusions may be caused by misidentification (Khurshid et al., 2004) and/or different Chinese dialects as well as different translations from the Chinese to English (Aradhya et al., 1995). To overcome the problem, molecular-level approaches have been used to discriminate genotypes, including isozyme fingerprinting (Aradhya et al., 1995), random amplified polymorphic DNA (Anuntalabhochai et al., 2002), microsatellite DNA (Viruel and Hormaza, 2004; Sun et al., 2012; Madhou et al., 2013), and single nucleotide polymorphism markers (Liu et al., 2015). However, it is very difficult for retailers, exporters, importers, and consumers to obtain the molecular genetic information needed to discriminate the cultivar origin of postharvest fruits. Because litchi cultivars can be described in terms of cultivar-dependent fruit appearance and several fruit characteristics (Menzel et al., 2005), the cultivar discrimination of postharvest fruits itself may be desirable, especially for consumers in countries that rely mainly on imported litchi fruit such as Japan. Traditionally, morphological traits such as fruit shape, appearance, and harvest season were used to discriminate the genotypes of the fruits (Wu, 1998). As for fruit characteristics, not only fruit morphological index such as whole fruit shape (round, egg, oblong, ellipse or heart), fruit shoulder shape (smooth or uneven), fruit apex shape (round, obtuse, or pointed), fruit skin protuberance type (sharp pointed, wedge, obtuse, or smooth), but also fruit physiological index such as fruit weight, seed size, sugar contents, flesh recovery rate and maturation period were used to describe litchi cultivars (Koul and Singh, 2017; Singh et al., 2012). The usefulness of this approach has been limited because these traits depend on environmental conditions (Khurshid et al., 2004). Thus, morphological traits have not been widely used as genotype indicators. However, the recently developed machine learning technology known as deep learning (DL) could enable us to establish models for precise image classification (Nasiri et al., 2019). DL provides a hierarchical representation of the data by means of various convolutions, which increases learning capabilities and thus performance and precision in image classification. However, little research has been reported on the discrimination of cultivars of litchi fruit images. In this study, we first investigated whether fruit appearance represents a cultivar-specific feature. For this purpose, we evaluated fruit shapes (fruit contours) quantitatively using elliptic Fourier descriptors (EFDs) and determined the differences in fruit shapes across different cultivars. Then, taking advantage of newly developed DL-based image recognition and processing technology, we developed a model to discriminate the cultivars in fruit images.

2. Materials and Methods

2.1. Plant materials

Litchi fruits were obtained from commercial fruit markets in Taipei city and an orchard located in Hsinchu city, Taiwan (24°46’37.0’’N, 120°58’21.3’’E) during the 2018 season. Mature fruits were harvested from the trees of four cultivars, ‘Gui Wei’ (GW), ‘Hei Ye’ (HY), ‘No Mai Tsz’ (NMT), and ‘Yu Her Pau’ (YHP), all of which are major cultivars in Taiwan (Chang et al., 2017). Smaller seed size, early harvesting period and greater sugar-to-acidity ratio in YHP (data not shown) were consistent with the cultivar description in Chang et al. (2017). Flesh recovery rate of NMT and YHP fruits were 78% whereas those of GW and HY fruits were 75% and 73%, respectively. Higher flesh recovery rate of NMT and YHP was also consistent with previous reports (Chang et al. 2017; Koul and Singh, 2017). HY fruits used in this study were heart-shaped with smooth fruit skin and without raised protuberances as described in Singh et al. (2012). YHP and HY, imported from Taiwan to Japan through a commercial retailing company, were also obtained during the 2019 season. Flesh recovery rate of YHP was 79%, higher than HY (74%), which was similar to the cultivar identification characteristics described in Chang et al. (2017) and the 2018 season samples. The fruits obtained in 2019 were used for further validation tests to evaluate the robustness of the developed classification model in this study.

2.2. Acquisition of fruit appearance images

The image data were taken by a digital camera (Nikon D7100). To photograph all fruits under the same conditions, they were placed on a black sheet and illuminated with an LED light. Two pictures were taken, one from the suture-line side and one from the opposite side (the non-suture-line side), of each fruit (Fig. 1).

2.3. Comparison of the quantitative descriptions of fruit shapes and colors across litchi cultivars

We selected 10 fruits of each cultivar that were free from any abnormal features in appearance. We used the SHAPE program (Iwata and Ukai, 2002) to evaluate the fruit shapes quantitatively. Two images were taken of 10 fruits; thus, a total of 20 fruit images were obtained for each cultivar tested in this study. In total, 80 fruit images were used for the quantitative evaluation of fruit contours and colors.

The SHAPE program converts color images into binary images based on a default settings. From these binary images, the closed contours of the samples were extracted and converted into a chain code (Freeman, 1974). The EFD coefficients were then calculated using the chain code data (Kuhl and Giardina, 1982), and we approximated the shape of each fruit using the first 20 harmonics. Thus, we calculated 80 (20×4) standardized EFDs per sample. Then, Principal Component Analysis (PCA) was conducted to summarize the information contained in these EFD coefficients. To determine the shape represented by each principal component (PC), we recalculated the EFD coefficients with the score of a particular PC equal to the mean ± 2 standard deviations (SD) while using the means of the remaining components. Finally, we used these PC scores for an analysis of variance (ANOVA) and identified the PCs with significant differences among cultivars. Those PCs (suture-line side: PC1 and PC2; non-suture-line side: PC1, PC2, PC4, and PC5) were used to evaluate the relationship between cultivars and fruit shapes. All of the calculation and statistical analysis were completed using the SHAPE program ver. 1.3 (Iwata and Ukai, 2002) and R ver. 3.5.2 (R Core Team, 2018).

The RGB color index was extracted from each fruit image. The RGB image was divided into three grayscale 8-bit images (Red, Green, and Blue) by 'split channels' function of Image J (Rasband, 2012). The mean gray value from each image was used to evaluate the relationship between cultivars and fruit colors.

2.4. Model construction using a convolutional neural network and model validation

To construct a deep convolutional neural network (CNN) model, we used the Keras platform (Chollet, 2015), which is a well-known neural network application programming interface based on Python ver. 3.6 and TensorFlow ver. 1.13.1 (Abadi et al., 2015). It was run under an Ubuntu 18.04 operating system.

We used 110 images of each cultivar, so a total of 440 images were processed.

The test fruit images in each cultivar were randomly divided into three subsets: a training data set, validation data set, and test data set. Eighty fruit images of each cultivar were used for training, 15 images were used for validation, and the remaining 15 images were reserved for final accuracy verification. Before the model was constructed, data augmentation was applied using ImageDataGenerator, which is an optional function in Keras (Chollet, 2015). The number of images in the training dataset was increased by shift along the X- and Y-axes, vertical and horizontal flip, zoom in, zoom out, and rotation of the images.

To develop the litchi cultivar discrimination model, we employed a fine-tuning method based on a VGG16 (Simonyan and Zisserman, 2014) that was pre-trained on the ImageNet data set. The model was trained with RGB image data 256 × 256 pixels in size. VGG16 initialized the network weights and transferred the learned features to a new task so that the parameters of the model were continuously updated by our litchi fruit image dataset. VGG16 consists of 13 convolutional layers with 3 × 3 kernels and five 2 × 2 max-pooling layers (Simonyan and Zisserman, 2014), which implement the transformation of data in a deep CNN. The model was validated through statistical parameters such as accuracy and loss. For model validation, the images not used for training were evaluated the percentage of correct and incorrect classifications were counted. Fifty each of the

2019 season YHP and HY fruit images from the imported fruits were classified for further model validation.

2.5. Model performance evaluation by Grad-CAM

To evaluate the classification performance of the model, the last layer before the final layer was extracted. Using the Gradient-weighted Class Activation Mapping (Grad-CAM) technique, areas used to extract features for the prediction of cultivar classes in each image were visualized by a heatmap (Selvaraju et al., 2017).

3. Results

3.1. Description of litchi fruit shapes using SHAPE

The SHAPE program was used to describe the fruit shape of each image. After PCA analysis, 6 and 5 PCs were obtained from the image on the suture-line and non-suture-line side, respectively (data not shown). ANOVA ($p < 0.05$) test revealed that PC1 and PC2 from suture-line side and PC1, PC2, PC4, and PC5 from non-suture line side showed significant differences among four cultivars (Fig. 2). Thus, this program detected several significant differences in fruit shapes across cultivars. Each suture-line side PC1 mean score (± SE) was -0.06546 (± 0.01058), -0.01306 (± 0.00730), -0.02881 (± 0.00933), and 0.10712 (± 0.01146) for GW, HY, NMT and YHP, respectively. Each non-suture-line side PC1 mean score (± SE) was 0.08211 (± 0.01142), 0.03063 (± 0.01088), 0.01529 (± 0.01346), -0.12792 (± 0.01418) for GW, HY, NMT and YHP, respectively. The PC1 scores from suture-line side and non-suture-line side are much higher and lower, respectively, in YHP compared to other cultivars. PC1 from both suture-line and non-suture-line sides mainly represents length-to-diameter ratio (Fig. 2), which suggests that YHP fruits tend to have higher LD ratio than other cultivars. Among PCs with significant difference across cultivars, PC1 represents fruit length-to-diameter (LD) ratio and accounts for more than 60% of the contribution. Although other PCs also had significant differences across cultivars, these differences could not be easily perceived by the naked eye, such as the difference in fruit width in lower lateral side as indicated in PC2 (Fig. 2). These results suggest that the SHAPE program can detect not only major fruit shape differences but also several minor fruit shape differences that are not easy for humans to see. To evaluate the relationship between fruit shapes and cultivars, PCA was conducted using all PCs with significant difference among cultivars. As shown in Fig. 3, all YHP fruits tend to be grouped together and have a distant relationship with other cultivars, which suggests that YHP may be unique in terms of fruit shape among 4 cultivars tested in this study. For other 3 cultivars, although GW and NMT tended to be grouped together, HY fruits were mixed together with some GW and NMT fruits. Thus, our fruit shape analysis suggested HY, GW and NMT have relatively close relationships with each other in terms of fruit shape. On the other hand, we also evaluated the relationship between fruit color and cultivars. In contrast to fruit shape, cultivar-dependent fruit color tendency was not found, suggesting that fruit color itself may not be as much effectively used for cultivar discrimination in litchi as fruit contour (Fig. S1).

3.2. Image recognition by DL and construction of the cultivar discrimination model

For the proposed cultivar discrimination model, the accuracy and loss values of training and validation at each epoch are shown in Fig. 4. The curves of validation accuracy and loss during training and validation reached a plateau after approximately 70 epochs. Moreover, when 68 epochs were used for each training session, the validation accuracy and loss were 1.0000 and 0.0046, respectively (Fig. 4). To evaluate the performance of the constructed model (epochs = 68), cultivar discrimination accuracy was evaluated using the test image dataset. Overall, the fruit images were classified as one of four cultivars with 98.33% accuracy (Table 1). The GW, NMT, and YHP images were correctly classified with an accuracy of 100%. In contrast, one of HY images was misclassified as GW.

We further tested whether this model discriminates the images of fruits collected from a different year and location (the 2019 season YHP and HY images). In this validation, 50 images were selected randomly from each cultivar. All YHP images were recognized as YHP (50/50). For HY images, the model correctly identified 82% of the HY fruits (41/50), and the remaining nine fruit images were recognized as GW (7/50) or YHP (2/50).

3.3. Evaluation of the model by Grad-CAM

A visualization of the prediction of correctly classified and misclassified fruit images was obtained using Grad-CAM (Selvaraju et al., 2017). In the case of correctly classified images, our discrimination model recognized the region of the fruit itself in the images (Figs. 5A, B, C, and D). Interestingly, the area of focus of the model was similar within a cultivar but different across cultivars. The model recognized whole areas of HY fruits, whereas specific areas were the focus for other cultivars. The main recognition areas of GW, NMT, and YHP were shoulder, lower lateral, and apex areas, respectively (Fig. 5). In misclassified images, the model recognized shoulder and background areas of HY fruit images, which may have caused the HY fruit to be misclassified as GW (Fig. 5 E)

4. Discussion

In this study, the fruit images of four major litchi cultivars in Taiwan were acquired and used for image analysis. First, we quantitatively evaluated litchi fruit shape using EFDs and characterized the relationship between cultivars and fruit shapes. We also employed DL for image recognition and developed a model to discriminate the cultivars of litchi fruit from images.

4.1. Characterization of cultivar-dependent fruit shapes using EFDs and PCA analysis

Fourier descriptors and statistical approaches have been used to discriminate biological objects including fruits such as oranges (Costa et al., 2009), apples (Currie et al., 2000), tomatoes (Visa et al., 2014), and persimmons (Maeda et al., 2018) on the basis of the morphological differences in their contours. Here, the EFDs of each fruit image were obtained and PCA analysis was performed. Our analysis suggests that, of the four cultivars, YHP has most distant relationship with other three cultivars, whereas HY have fruit shapes that are similar to NMT and GW (Fig. 3). In fact, many YHP fruit had an oblong shape whereas the other cultivars had round shapes (Fig. 1). Thus, EFDs could describe each litchi fruit shape precisely and quantitatively. Moreover, some fruit contours represent cultivar-specific features in litchi.

4.2. Our DL image recognition method to discriminate cultivars of fruit images

To consider not only fruit contours but also whole fruit appearance factors such as peel color and texture for cultivar discrimination, we employed DL using a deep CNN in this study. In this approach, intact RGB fruit images are recognized. The VGG16 architecture was fine-tuned to construct a cultivar discrimination model. To do this, we used the non-suture-line side images (Fig. 1-ii) because they showed more fruit shape differences across cultivars than suture-line side images (Fig. 2). We successfully developed a model to discriminate cultivars of fruit images with 98.33% accuracy. Moreover, we demonstrated that this model could identify YHP fruits collected from different season with 100% accuracy and HY fruits with 82% accuracy, which suggests that the model using DL image recognition technology can identify genotype-dependent litchi fruit images, especially for YHP fruits.

Grad-CAM (Selvaraju et al., 2017) revealed that our model was well trained because it recognizes similar regions within the same cultivars and different regions across the cultivars (Fig. 5), which may increase the accuracy of a cultivar discrimination model. DL-based fruit quality classification has been previously proposed in agriculture and fishery research. For instance to assess the fruit quality of dates (*Pheonix dactylifera* L.), more than 1,300 images were used to develop a classification model that had a validation accuracy and loss of 0.9846 and 0.0522, respectively (Nasiri et al., 2019). A shrimp quality recognition model was developed using more than 10,000 images (Liu, 2020), and three different squid classification models were developed using 600 images (Hu et al., 2020). Our model, in contrast, used only 380 images for training and could discriminate for cultivars with values of 1.0000 and 0.0046 for the validation accuracy and loss, respectively (Fig. 4), which are higher and lower, respectively, than the date fruit quality classification model (Nasiri et al., 2019). This implies that the litchi fruit appearance tested in this study may contain distinct cultivar-dependent characteristics, such as variation of local skin color and texture, which might enable us to construct high-accuracy cultivar classification model using fewer training images.

However, our classification model classified one HY fruit image as a GW image (Table 1) and could not recognize 18% of HY fruit images collected from different years and sites. The Grad-CAM analysis suggests that the model focused on the shoulder region in misclassified images, which is the typical region of focus for GW (Fig. 5). Indeed, our analysis on fruit shapes suggested that HY may have close relationship with other cultivars in terms of fruit shapes (Fig. 3). Therefore, although our CNN model may potentially be capable of discriminating litchi cultivars using RGB fruit images, further model improvement will be required for practical use. SHAPE analysis conducted in this study suggested that fruit contour represents minor but significant differences among cultivars (Fig. 2). On the other hand, the Grad-CAM analysis suggests that our model might not use fruit contour effectively for cultivar discrimination (Fig. 5). Thus, combined use of cultivar-dependent fruit contour and fruit inside structures such as texture and color may possibly improve our model. The Grad-CAM analysis further suggests that, in the case of misclassified fruit images, the model tends to consider non-fruit areas for cultivar discrimination (Fig. 5). Therefore, training with a higher number of fruit images and using fruit images with various backgrounds may be another appropriate strategy to improve our model.

5. Conclusion

The aim of this study was to develop a cultivar discrimination model for litchi fruit images. We first characterized fruit shape diversity across cultivars using EFDs and PCA analysis. Our fruit shape characterization revealed that YHP can be easily discriminated from other cultivars due to its higher length-to-diameter ratio. We then employed DL to discriminate litchi cultivars. Intact RGB fruit images were recognized using DL based on VGG16, which is a CNN architecture. As a result, we developed a cultivar discrimination model with high accuracy. This is the first report that DL can be effectively applied for litchi fruit image recognition and cultivar discrimination. Our model perfectly recognized YHP fruit images collected from a different season and location. Furthermore, Grad-CAM visualization analysis suggests a relatively small number of images are sufficient to train the model to discriminate cultivars with high accuracy. However, further model evaluation and improvement will be necessary for practical use. The model accuracy should be further evaluated by using more images of fruits collected in different climate, cultural practices and ripening stages. To expand the model to other cultivars in future, model improvement will be required especially when discriminating the fruit images of cultivars that look very similar.

Acknowledgments

GW, HY, and NMT fruit samples in 2018 season were kindly provided from Mr. Wang's orchard located in Hsinchu city, Taiwan. We thank Kimberly Moravec, PhD, from Edanz Group (www.edanzediting.com/ac) for editing a draft of this manuscript.

References

Abadi, M., Agarwal, A., Barham, P., Brevdo, E., Chen, Z., Citro, C., Corrado, G.S., Davis, A., Dean, J., Devin, M., Ghemawat, S., Goodfellow, I., Harp, A., Irving, G., Isard, M., Jia, Y., Jozefowicz, R., Kaiser, L., Kudlur, M., Levenberg, J., Mané, D., Monga, R., Moore, S., Murray, D., Olah, C., Schuster, M., Shlens, J., Steiner, B., Sutskever, I., Talwar, K., Tucker, P., Vanhoucke, V., Vasudevan, V., Viégas, F., Vinyals, O., Warden, P., Wattenberg, M., Wicke, M., Yu, Y., Zheng, X., 2016. TensorFlow: Large-Scale Machine Learning on Heterogeneous Distributed Systems. https://arxiv.org/abs/1603.04467

Anuntalabhochai, S., Chundet, R., Chiangda, J., Apavatjrut, P., 2002. Genetic diversity within Lychee (*Litchi chinensis* Sonn.) based on RAPD analysis. Acta Hortic. 575, 253-259. https://doi.org/10.17660/ActaHortic.2002.575.27

Aradhya, M.K., Zee, F.T., Manshardt, R.M., 1995. Isozyme variation in lychee (*Litchi chinensis* Sonn.). Sci. Hortic. (Amsterdam). 63, 21–35. https://doi.org/10.1016/0304-4238(95)00788-U

Chang, C., 1961. The lychee growing in Taiwan. J. Agric. Assoc. China1. 33, 51–63.

Chang, J., Cheng, Y., Yen, C., Hsu, H., Chao, C., Tien, Y., Ho, C., Lin, C., 2005. A new variety of litchi (*Litchi chinensis* Sonn.) Tainung NO. 1. J. Taiwan Agric. Res. 54, 43–53. http://dx.doi.org/10.6730/JAAT.200902_10(1).0006

Chang, J.W., Chen, P.A., Chen, I.Z., 2017. Litchi breeding and plant management in Taiwan, in: Kumar, M., Kumar, V., Prasad, R., Varma, A. (Eds.), The Lychee Biotechnology. Springer, Singapore, pp. 31-58. https://doi.org/10.1007/978-981-10-3644-6_2

Chang, JC, Lin, T., Yen, C., Chang, JW, Lee, W., 2009. Litchi production and improvement in Taiwan. J. Agric. Assoc. Taiwan. 10, 63–67.

Chollet, F., 2015. Keras. https://github.com/keras-team/keras (accessed 15 November 2019)

Costa, C., Menesatti, P., Paglia, G., Pallottino, F., Aguzzi, J., Rimatori, V., Russo, G., Recupero, S., Reforgiato Recupero, G., 2009. Quantitative evaluation of Tarocco sweet orange fruit shape using optoelectronic elliptic Fourier based analysis. Postharvest Biol. Technol. 54, 38–47. https://doi.org/10.1016/j.postharvbio.2009.05.001

Currie, A.J., Ganeshanandam, S., Noiton, D.A., Garrick, D., Shelbourne, J.A., Oraguzie, & N., 2000. Quantitative evaluation of apple (*Malus* × *domestica* Borkh.) fruit shape by principal component analysis of Fourier descriptors, Euphytica. 111, 221-227. https://doi.org/10.1023/A:1003862525814

Freeman, H., 1974. Computer Processing of Line-Drawing Images. ACM Comput.

Surv. 6, 57-97. https://doi.org/10.1145/356625.356627

Hu, J., Zhou, C., Zhao, D., Zhang, L., Yang, G., Chen, W., 2020. A rapid, low-cost deep learning system to classify squid species and evaluate freshness based on digital images. Fish. Res. 221, 105376. https://doi.org/10.1016/j.fishres.2019.105376

Huang, X., Subhadrabandhu, S., Mitra, S.K., Ben-Arie, R., Stern, R.A., 2005. Origin, history, production and processing., in: Litchi and Longan: Botany, Production and Uses. https://doi.org/10.1079/9780851996967.0001

Iwata, H., Ukai, Y., 2002. SHAPE: a computer program package for quantitative evaluation of biological shapes based on elliptic Fourier descriptors. J. Hered. 93, 384-385. https://doi.org/10.1093/jhered/93.5.384

Koul, B., Singh, J., 2017. Lychee biology and biotechnology, in: Kumar, M., Kumar, V., Prasad, R., Varma, A. (Eds.), The Lychee Biotechnology. pp. 137–192. https://doi.org/10.1007/978-981-10-3644-6Khurshid, S., Ahmad, I., Anjum, M.A., 2004. Genetic diversity in different morphological characteristics of litchi (*Litchi chinensis* Sonn.). Int. J. Agric. Biol. 6, 1062–1065.

Kuhl, F.P., Giardina, C.R., 1982. Elliptic Fourier features of a closed contour. Comput. Graph. Image Process. 18, 236-258. https://doi.org/10.1016/0146-664X(82)90034-X

Liu, W., Xiao, Z., Bao, X., Yang, X., Fang, J., Xiang, X., 2015. Identifying Litchi (*Litchi chinensis* Sonn.) cultivars and their genetic relationships using single nucleotide polymorphism (SNP) markers. PLoS One. 10, e0135390. https://doi.org/10.1371/journal.pone.0135390

Liu, Z., 2020. Soft-shell Shrimp Recognition Based on an Improved AlexNet for Quality Evaluations. J. Food Eng. 266, 109698. https://doi.org/10.1016/j.jfoodeng.2019.109698

Madhou, M., Normand, F., Bahorun, T., Hormaza, J.I., 2013. Fingerprinting and analysis of genetic diversity of litchi (*Litchi chinensis* Sonn.) accessions from different germplasm collections using microsatellite markers. Tree Genet. 9, 387-396. Genomes. https://doi.org/10.1007/s11295-012-0560-1

Maeda, H., Akagi, T., Tao, R., 2018. Quantitative characterization of fruit shape and its differentiation pattern in diverse persimmon (*Diospyros kaki*) cultivars. Sci. Hortic. (Amsterdam). 228, 41-48. https://doi.org/10.1016/j.scienta.2017.10.006

Menzel, C.M., Huang, X., Liu, C., 2005. Cultivars and plant improvement., in: Litchi and Longan: Botany, Production and Uses. https://doi.org/10.1079/9780851996967.0059

Mitra, S.K., Pathak, P.K., 2010. Litchi production in the Asia-Pacific region. Acta

Hortic. 863, 29-36. https://doi.org/10.17660/ActaHortic.2010.863.1

Nasiri, A., Taheri-Garavand, A., Zhang, Y.D., 2019. Image-based deep learning automated sorting of date fruit. Postharvest Biol. Technol. 153, 133-141. https://doi.org/10.1016/j.postharvbio.2019.04.003

Rasband, W.S., 2012. ImageJ: Image processing and analysis in Java. Astrophysics Source Code Library.

Selvaraju, R.R., Cogswell, M., Das, A., Vedantam, R., Parikh, D., Batra, D., 2017. Grad-CAM: Visual Explanations from Deep Networks via Gradient-based Localization. http://arxiv.org/abs/1610.02391

Simonyan, K., Zisserman, A., 2014. Very Deep Convolutional Networks for Large-Scale Image Recognition. http://arxiv.org/abs/1409.1556

Singh, G., Nath, V., Pandey, S.D., Ray, P.K., 2012. Cultivars and genetic enhancement, in: Food and agriculture organization of the united nations (FAO) (Ed.), The litchi. New Delhi, pp. 18-35. http://tmnehs.gov.in/forms/MainLink.aspx?lid=1003&Id=32

Sun, Q., Bai, L., Ke, L., Xiang, X., Zhao, J., Ou, L., 2012. Developing a core collection of litchi (*Litchi chinensis* Sonn.) based on EST-SSR genotype data and agronomic traits. Sci. Hortic. (Amsterdam). 146, 29-38.

https://doi.org/10.1016/j.scienta.2012.08.012

Taiwan Agricultural Statistic Year Book, 2015. Council of agriculture, Taipei.

R core team, 2018. R: A language and environment for statistical computing. R Foundation for Statistical Computing, Vienna, Austria. http://www.R-project.org

Viruel, M.A., Hormaza, J.I., 2004. Development, characterization and variability analysis of microsatellites in lychee (*Litchi chinensis* Sonn., Sapindaceae). Theor. Appl. Genet. 108, 896-902. https://doi.org/10.1007/s00122-003-1497-4

Visa, S., Cao, C., Gardener, B.M.S., van der Knaap, E., 2014. Modeling of tomato fruits into nine shape categories using elliptic fourier shape modeling and Bayesian classification of contour morphometric data. Euphytica 200, 429–439. https://doi.org/10.1007/s10681-014-1179-0

Wu, S., 1998. Encyclopedia of china fruits: litchi. China Forestry Press, Beijing.

Table 1. Discrimination accuracy for images not used for model construction.

		Predicted cultivars			
		GW	HY	NMT	YHP
True cultivars	GW	15	0	0	0
	HY	1	14	0	0
	NMT	0	0	15	0
	YHP	0	0	0	15

Figure legends

Figure 1. Examples of images of each cultivar. A: GW. B: HY. C: NMT. D: HYP. i: Fruit image taken from the suture-line side. ii: Fruit image taken from non-suture-line side. The scale bar indicates 1cm. Each fruit was placed under the direction of stem end at upper side and fruit apex at lower side. Arrows indicate suture lines of each fruit.

Figure 2. Fruit shape diversities in suture-line side and opposite (non-suture-line) side images as visualized by contours based on PCs that show significant differences across cultivars based on ANOVA ($p < 0.05$). Each shape was reconstructed from the EFD coefficients, which were calculated using the score for a PC equal to the mean ± 2 SD. Percentages indicate the contribution rates of each PC and *p* indicates the *p*-value of each PC for the ANOVA result across cultivars. Each fruit shape was drawn under the direction of stem end at upper side and fruit apex at lower side.

Figure 3. PCA plot of analysis using all PCs with significant difference in fruit contour among 4 cultivars based on SHAPE program and ANOVA ($p < 0.05$). Each ellipse indicates the normal confidence ellipse of each cultivar at a level of 0.95 confidence.

Figure 4. Classification accuracy (A) and loss (B) over 150 training epochs.

Figure 5. Prediction visualization using the Grad-CAM technique. Here, the "block5_conv3" layer is visualized as a heatmap. Warm colors suggest that the region more strongly contributes to the prediction. A: GW image predicted as GW, B: HY image predicted as HY, C: NMT image predicted as NMT, D: YHP image predicted as YHP, E: HY image predicted as GW. i: RGB image inputted to the CNN model. ii: Heat-map image created by the Grad-CAM technique. Each fruit was places under the direction of stem end at upper side and fruit apex at lower side.

Figure S1. The relationship between fruit color and cultivars. 'Red_Mean' and 'Green_Mean' values indicate gray-scale value obtained from 8-bit red and green images, respectively, generated by ImageJ software.

Figure 1

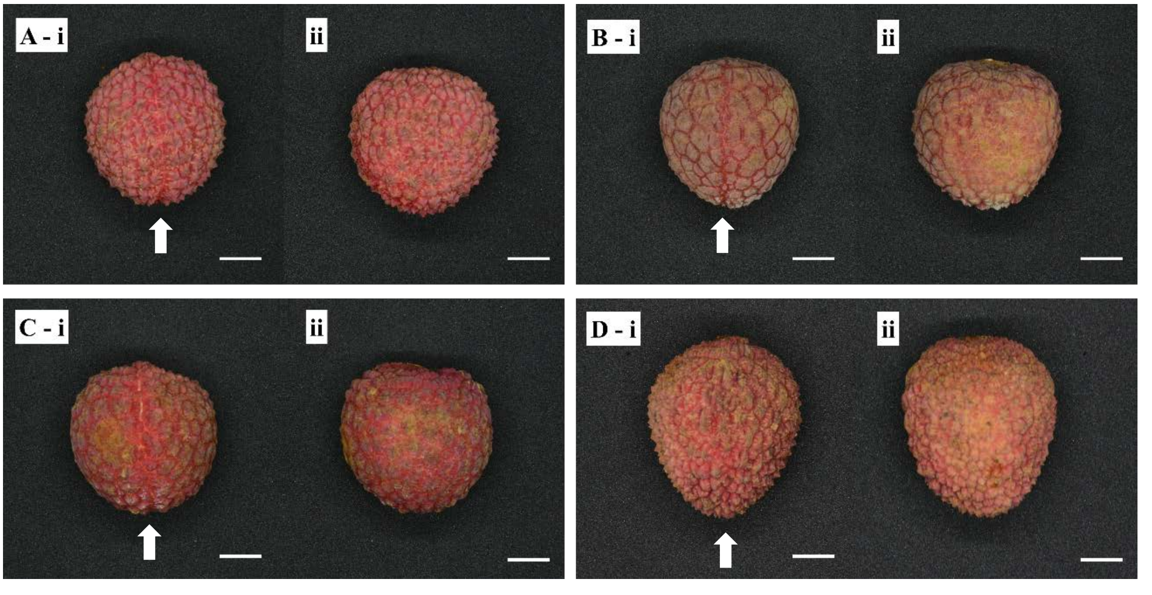

Figure 2

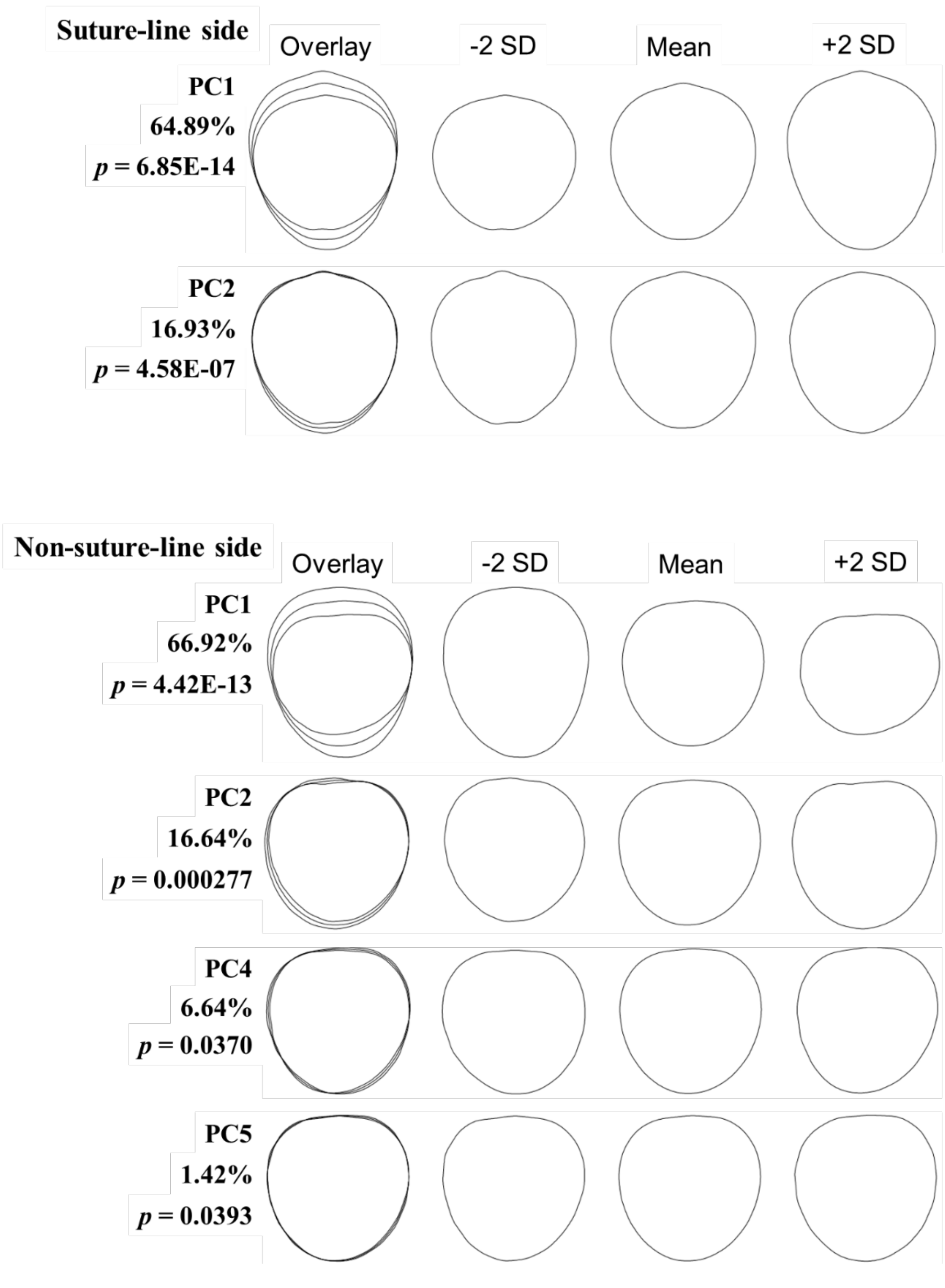
Suture-line side
Overlay
-2 SD
Mean
+2 SD
PC1
64.89%
p = 6.85E-14
PC2
16.93%
p = 4.58E-07
Non-suture-line side
Overlay
-2 SD
Mean
+2 SD
PC1
66.92%
p = 4.42E-13
PC2
16.64%
p = 0.000277
PC4
6.64%
p = 0.0370
PC5
1.42%
p = 0.0393

Figure 3

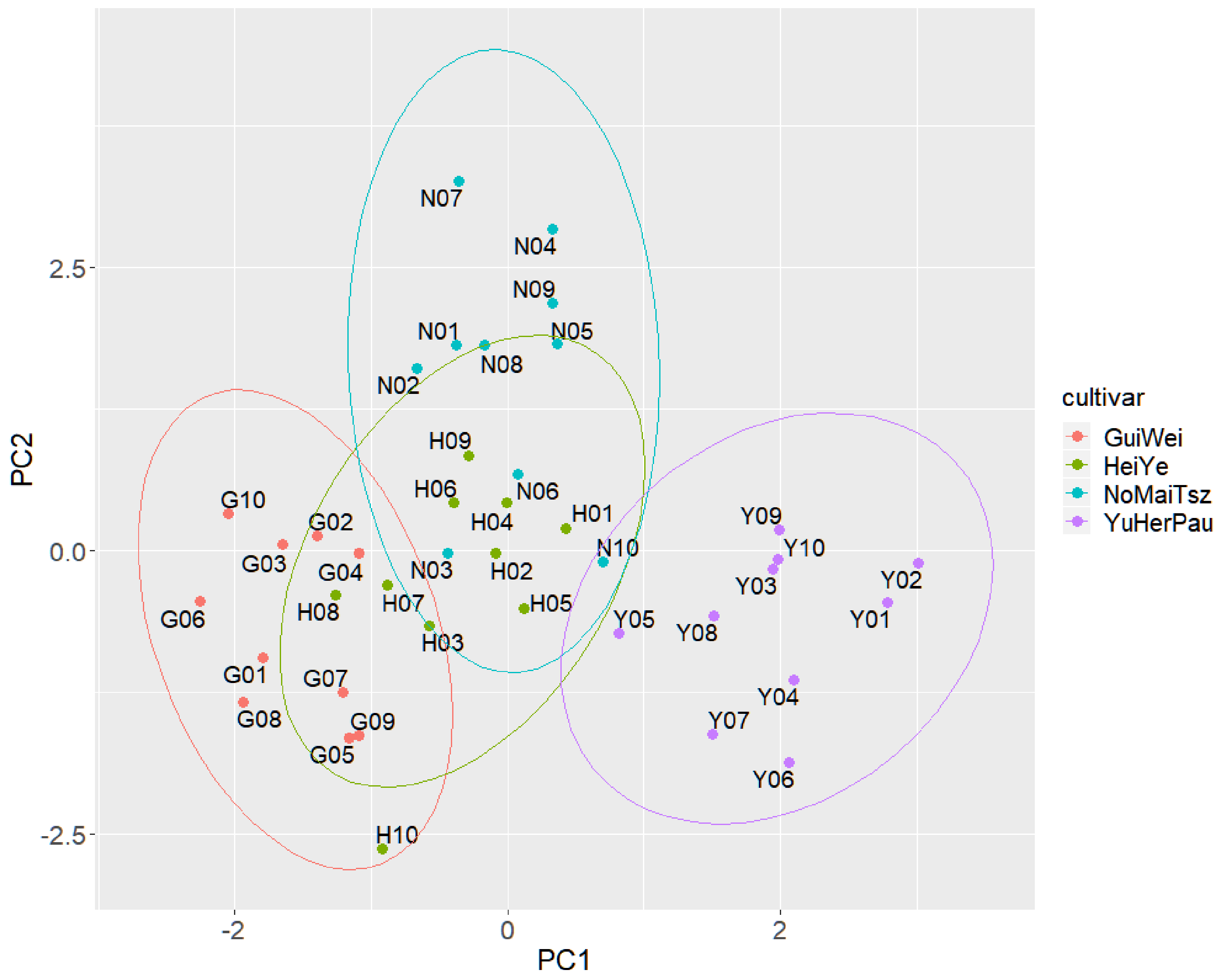

PC2
2.5
0.0
-2.5
-2
0
2
PC1
N07
N04
N09
N01
N05
N08
N02
H09
H06
N06
H04
H01
G10
G02
G03
G04
N03
H02
N10
G06
H08
H07
H05
H03
G01
G07
G08
G09
G05
H10
Y09
Y10
Y03
Y02
Y05
Y08
Y01
Y04
Y07
Y06
cultivar
GuiWei
HeiYe
NoMaiTsz
YuHerPau

Figure 4

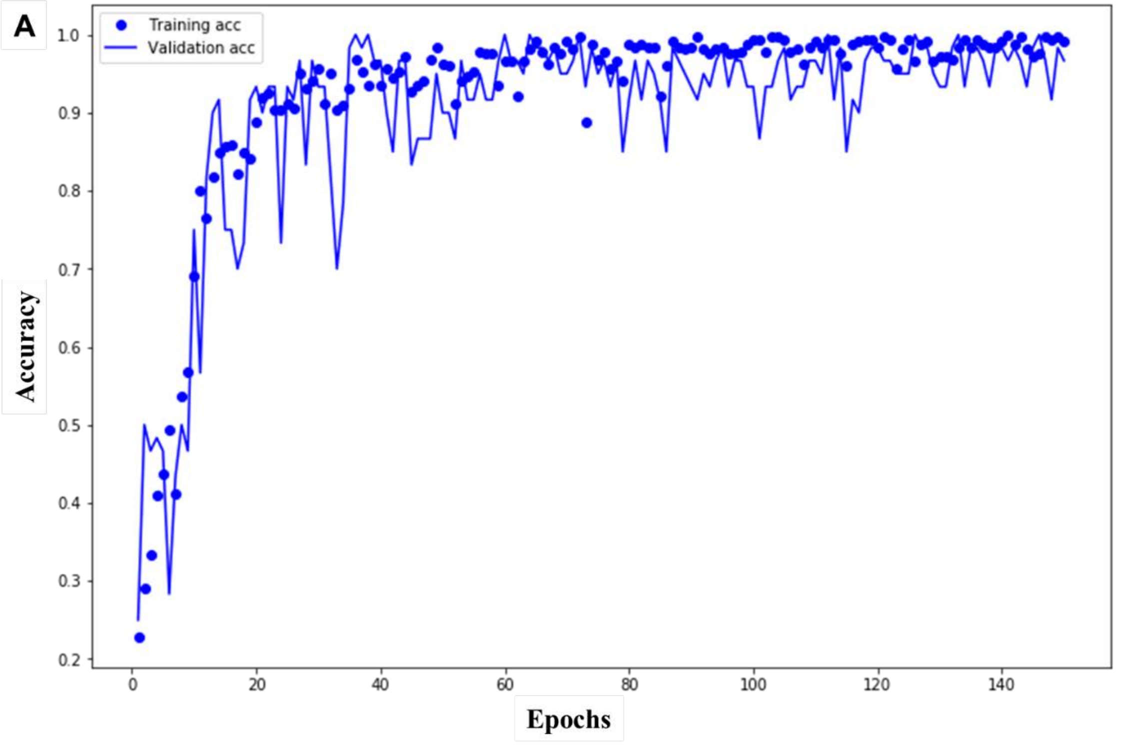

A
Training acc
Validation acc
Accuracy
Epochs

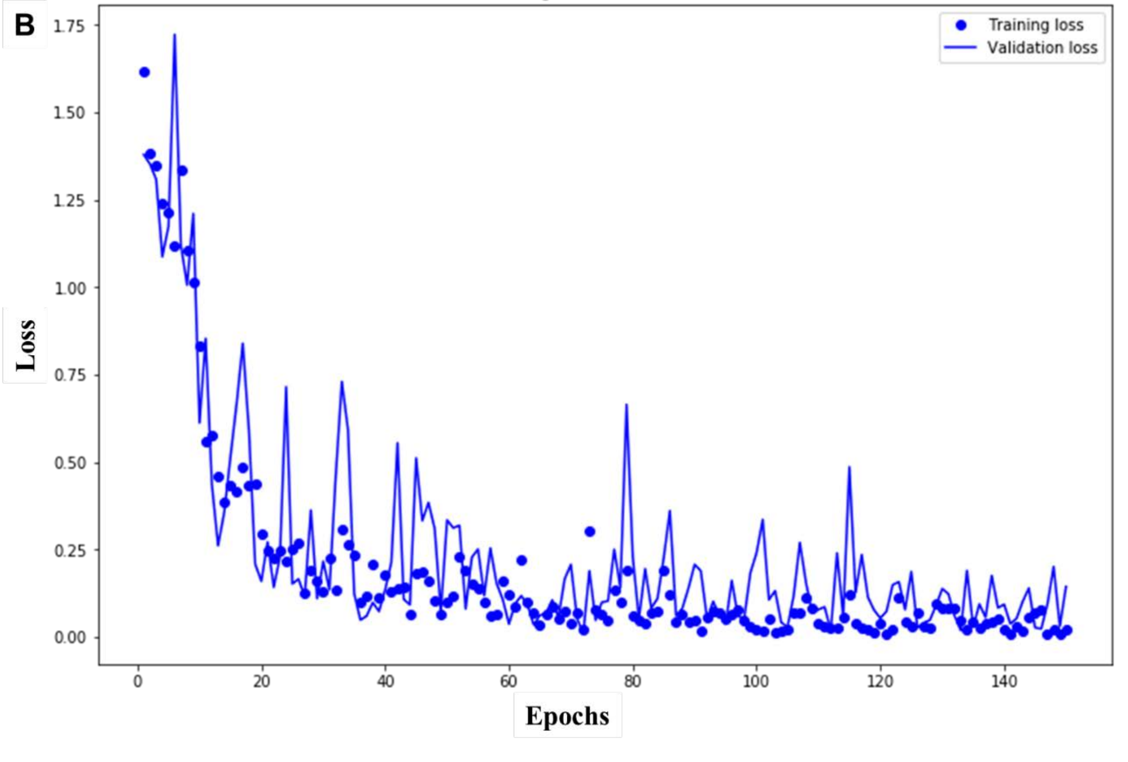

B
Training loss
Validation loss
Loss
Epochs

Figure 5

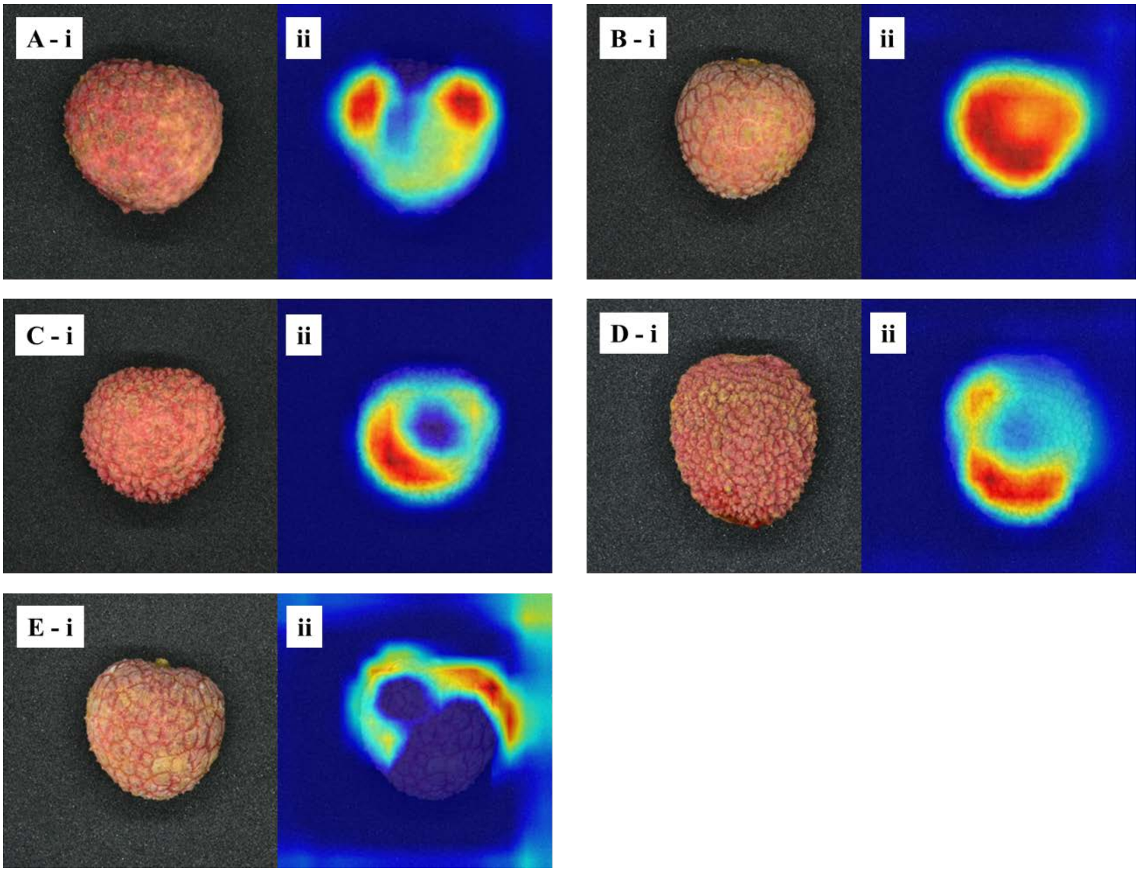

Figure S1

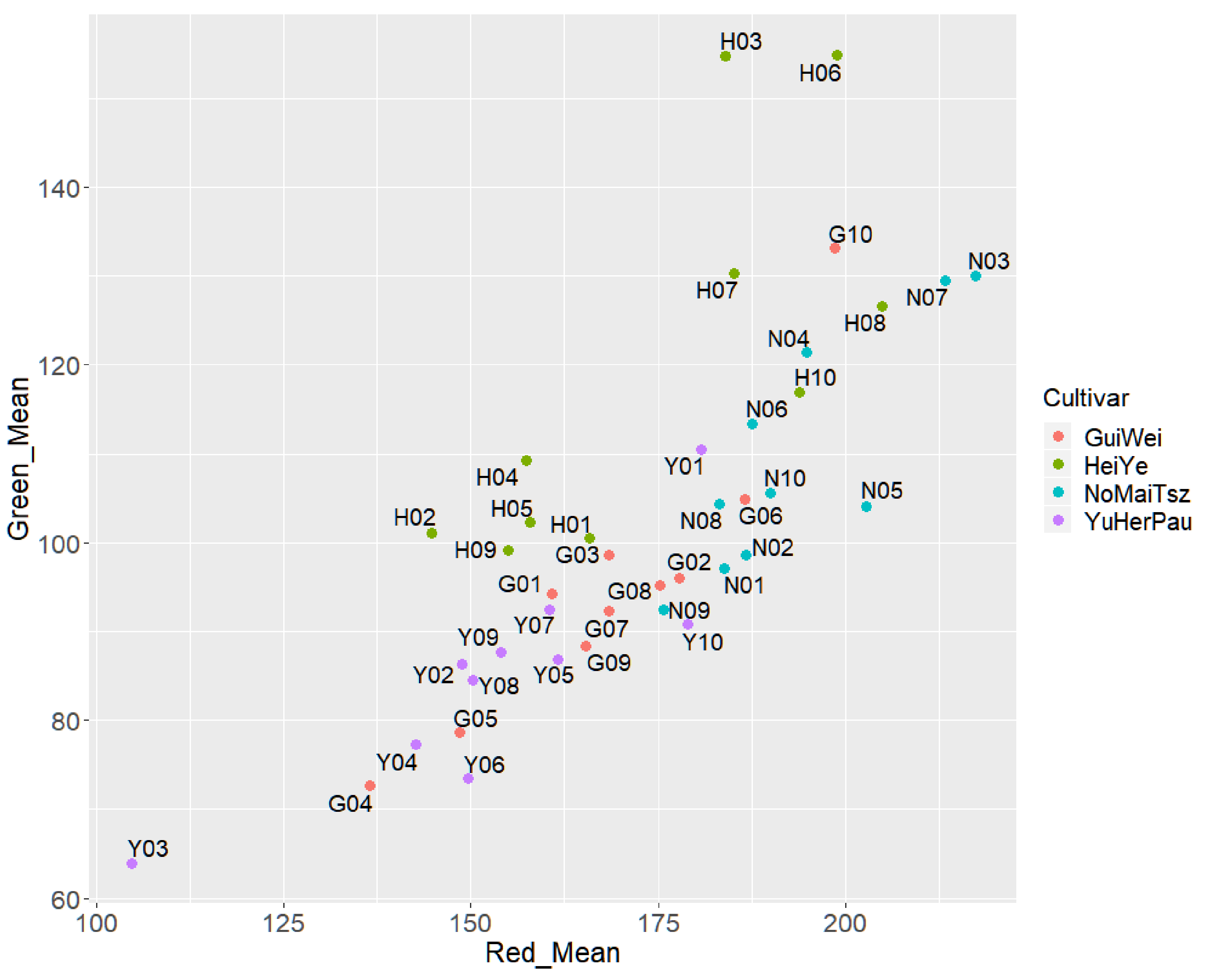

Green_Mean
Red_Mean
140
120
100
80
60
100
125
150
175
200
Cultivar
GuiWei
HeiYe
NoMaiTsz
YuHerPau
H03
H06
G10
N03
H07
N07
H08
N04
H10
N06
Y01
H04
N10
N05
H05
H01
N08
G06
H02
H09
G03
N02
G02
N01
G01
G08
N09
Y07
G07
Y10
Y09
G09
Y02
Y05
Y08
G05
Y04
Y06
G04
Y03